Editors' Suggestion

Correlation-induced orbital angular momentum changes

Yongtao Zhang,[1,2] Olga Korotkova,[3] Yangjian Cai,[4,5,*] and Greg Gbur[2,†]

[1]*College of Physics and Information Engineering, Minnan Normal University, Zhangzhou 363000, China*

[2]*Department of Physics and Optical Science, University of North Carolina at Charlotte, Charlotte, North Carolina 28277, USA*

[3]*Department of Physics, University of Miami, Coral Gables, Florida 33146, USA*

[4]*Shandong Provincial Engineering and Technical Center of Light Manipulations and Shandong Provincial Key Laboratory of Optics and Photonic Device, School of Physics and Electronics, Shandong Normal University, Jinan 250358, China*

[5]*School of Physical Science and Technology, Soochow University, Suzhou 215006, China*

(Received 4 May 2020; revised 2 November 2020; accepted 9 November 2020; published 9 December 2020)

We demonstrate that the orbital angular momentum (OAM) flux density of a paraxial light beam can change on propagation in free space. These changes are entirely due to the spatial coherence state of the source, and the effect is analogous to correlation-induced changes in the intensity, spectrum, and polarization of a beam. The use of the source coherence state to control the width, shape, and transverse shifts of the OAM flux density is demonstrated with numerical examples.

DOI: 10.1103/PhysRevA.102.063513

I. INTRODUCTION

Over the development of the theory of optical coherence, it has been increasingly appreciated that the state of spatial coherence can influence a number of fundamental properties of a light beam on propagation in free space, without any interactions with a medium. The earliest example of this was introduced in work by Collett and Wolf in 1978, in which they demonstrated that the diffraction rate of a partially coherent beam can be controlled by the source coherence state [1]. In the late 1980s, Wolf and colleagues caused a scientific furor when they showed that the spectrum of light can be changed on propagation due to source coherence [2,3], and can even under special circumstances mimic cosmological redshifts [4]. This revelation led to searches for other correlation-induced changes in light beams. In 1994, James demonstrated that source coherence may be responsible for changes in the degree of polarization [5], and in 2005 Korotkova and Wolf showed that the state of polarization may be similarly affected [6]. In this paper, we introduce another effect related to the source spatial coherence: correlation-induced changes in the orbital angular momentum flux density of light.

In recent years, there has been significant interest in the development of singular optics, as a relatively unexplored area of classical electromagnetism, for use in innovative technologies [7–9]. This research area largely focuses on optical vortices (singularities of wavefield phase), such as those which appear in Laguerre-Gauss beams of nonzero azimuthal order. These vortex beams are now known to possess orbital angular momentum (OAM), which is connected to the circulating phase of the vortex [10,11]. The OAM of light has already been applied to a number of applications, including optical trapping and rotation [12], the design of light-driven machines [13], and free-space optical communication [14,15].

The relationship between partial coherence and OAM has only recently been explored in significant detail. Early work demonstrated that optical vortices turn into vortices of the two-point correlation functions as the spatial coherence is decreased [16–18], suggesting that such structures are relatively robust. The OAM of partially coherent vortex beams, in particular the distribution of OAM flux in a beam's cross-section, was only investigated in 2012 [19], and it was shown that it generally manifests a Rankine vortex structure [20], with a core rotating like a rigid body and outskirts rotating like a fluid. In 2018, Gbur showed that there exist three fundamental classes of partially coherent vortex beams, characterized by their OAM distribution: rigid rotators, fluid rotators, and Rankine rotators [21].

In this paper, we show that one can use source correlations to change the OAM flux density of a beam on propagation in free space. These correlation-induced OAM changes can be significant and can be controlled by an appropriate choice of source correlations. Since the earlier work on correlation-induced spectral changes and polarization was done, coherence theory itself has evolved considerably, with alternative classes of correlation functions providing alternative effects and tunability. For example, it has been shown that structuring of the amplitude [22] or phase [23] of the source coherence state can result in controllable beam profiles, tilts, radial acceleration, or asymmetric splitting of a propagating beam. Here we derive the basic theory showing how source coherence results in unusual distributions of OAM flux density on propagation, and illustrate such changes with a number of source coherence models.

II. COHERENCE AND OAM

A scalar partially coherent beam in a plane perpendicular to the direction of propagation can be characterized by the cross-spectral density (CSD) function (see [24], Chap. 4),

$$W(\mathbf{r}_1, \mathbf{r}_2) = \langle U^*(\mathbf{r}_1) U(\mathbf{r}_2) \rangle_\omega, \tag{1}$$

*yangjiancai@suda.edu.cn

†gjgbur@uncc.edu

where $U(\mathbf{r})$ is the field at frequency ω, $\mathbf{r}_1$ and $\mathbf{r}_2$ are the transverse position vectors, and the angular brackets $\langle\cdots\rangle_\omega$ represent averaging over a space-frequency ensemble (see [24], Chap. 4).

The average OAM flux density $L_d(\mathbf{r})$ of such a beam can be shown to be related to the CSD by the expression [19]

$$L_d(\mathbf{r}) = -\frac{\epsilon_0}{k}\mathrm{Im}\left[\left(y_1\partial_{x_2} - x_1\partial_{y_2}\right)W(\mathbf{r}_1,\mathbf{r}_2)\right]_{\mathbf{r}_1=\mathbf{r}_2=\mathbf{r}}, \tag{2}$$

where $k = 2\pi/\lambda$ is the wave number of the light, with λ being the wavelength, and ϵ_0 is the free-space permittivity. Here ∂_{α_2} represents the partial derivative with respect to α_2, with $\alpha = x, y$.

The magnitude of the OAM flux density at a particular point in space arises from two distinct effects: the average OAM per photon and the density of photons in space, i.e., the intensity. We isolate the OAM of individual photons by considering the average normalized OAM flux density, defined as

$$l_d(\mathbf{r}) = \frac{\hbar\omega L_d(\mathbf{r})}{S(\mathbf{r})}, \tag{3}$$

where

$$S(\mathbf{r}) = \frac{k}{\mu_0\omega}W(\mathbf{r},\mathbf{r}) \tag{4}$$

is the z component of the Poynting vector. The dimensions of $l_d(\mathbf{r})$ are angular momentum per photon; the quantity therefore represents the average OAM of a photon measured at the particular position $\mathbf{r}$. For any Laguerre-Gauss mode of azimuthal order l, we have $l_d(\mathbf{r}) = l\hbar$, a constant.

We may also introduce the total OAM per photon t_d by the related formula

$$t_d = \frac{\hbar\omega\int L_d(\mathbf{r})d^2r}{\int S(\mathbf{r})d^2r}. \tag{5}$$

The quantity t_d remains constant on propagation, as total OAM is conserved; the quantity $l_d(\mathbf{r})$, however, may in general exhibit changes on propagation. We now demonstrate via example that it is possible to have OAM flux density changes that are entirely due to changes in the source coherence.

The CSD of a source in the plane $z = 0$ propagates in free space to a distance z via Fresnel diffraction:

$$W(\boldsymbol{\rho}_1,\boldsymbol{\rho}_2,z) = \frac{1}{(\lambda z)^2}\iint W(\mathbf{r}_1,\mathbf{r}_2) \times \exp\left\{-\frac{ik}{2z}[(\mathbf{r}_1-\boldsymbol{\rho}_1)^2 - (\mathbf{r}_2-\boldsymbol{\rho}_2)^2]\right\} \times d^2r_1 d^2r_2, \tag{6}$$

where $\boldsymbol{\rho}_1$ and $\boldsymbol{\rho}_2$ are the transverse position vectors at distance z.

We begin by considering isotropic Schell-model sources with a definite topological charge, of the form

$$W(\mathbf{r}_1,\mathbf{r}_2) = U_l^*(\mathbf{r}_1)U_l(\mathbf{r}_2)\mu_0(|\mathbf{r}_2-\mathbf{r}_1|), \tag{7}$$

where $\mu_0(|\mathbf{r}_2-\mathbf{r}_1|)$ is the spectral degree of coherence of the field with charge l, and the function $U_l(\mathbf{r})$ represents a vortex beam of radial order zero and azimuthal order l, expressed in polar coordinates (r,ϕ) as

$$U_l(\mathbf{r}) = C_l r^{|l|}\exp[il\phi]\exp\left[-\frac{r^2}{w^2}\right]. \tag{8}$$

In this expression, we have

$$C_l \equiv \sqrt{\frac{2}{\pi w^2|l|!}}\left(\frac{\sqrt{2}}{w}\right)^{|l|}, \tag{9}$$

with $\mathbf{r} = (r,\phi)$, and w is the initial beam width.

It is important to note that the spectral degree of coherence has no effect on the total OAM $t_d = l\hbar$ or the source distribution of OAM, i.e., $l_d(\mathbf{r}) = l\hbar$, as it is a homogeneous and isotropic function. If the field were fully coherent, $l_d(\mathbf{r})$ would also remain constant on propagation, but when the spatial coherence is changed $l_d(\mathbf{r})$ changes as well—any change observed in a partially coherent beam of the form of Eq. (7) is therefore entirely due to the effects of partial coherence.

III. EXAMPLES

To show the variety of changes possible, we consider a multi-Gaussian Schell-model vortex (MGSMV) source [22] with a source spectral degree of coherence

$$\mu_0(|\mathbf{r}_2-\mathbf{r}_1|) = \frac{1}{C_0}\sum_{m=1}^{\infty}\frac{(-1)^{m-1}}{m}\binom{M}{m}\exp\left[-\frac{|\mathbf{r}_1-\mathbf{r}_2|^2}{\delta_m^2}\right], \tag{10}$$

where

$$C_0 \equiv \sum_{m=1}^{\infty}\frac{(-1)^{m-1}}{m}\binom{M}{m} \tag{11}$$

is a normalization factor, $\binom{M}{m}$ is a generalized binomial coefficient which can take integer or fractional values of M [25], and $\delta_m = \sqrt{m}\delta$ are the correlation widths of the constituent Gaussian functions. For $M > 1$, this degree of coherence produces a flat-topped beam profile; for $M < 1$, it produces a cusped beam profile. For $M = 1$, this reduces to the traditional Gaussian Schell-model case, i.e.,

$$\mu_0(|\mathbf{r}_2-\mathbf{r}_1|) = \exp\left[-\frac{|\mathbf{r}_1-\mathbf{r}_2|^2}{\delta^2}\right], \tag{12}$$

where δ is the correlation width.

We consider the case $l = 1$; on substitution from Eq. (7) into Eq. (6), we can analytically evaluate the CSD at any propagation distance; expressions for the CSD, the OAM flux density, and the Poynting vector of an individual Gaussian Schell-model vortex beam are given in the Appendix.

Figure 1 shows the evolution of the normalized OAM flux density l_d of such MGSMV beams on propagation, for different orders M and different correlation widths δ. We take $\lambda = 632.8$ nm and $w = 1$ mm for the remainder of the paper. Figures 1(a) and 1(b) illustrate the effects of correlation width δ, with $M = 1$, the case of a Gaussian Schell-model beam. At small propagation distances, the beams act largely like fluid rotators—with near-constant $l_d(\mathbf{r})$ and a very small rigid body region in the core—and the rigid body region expands as it propagates. A beam with lower spatial coherence (smaller δ)

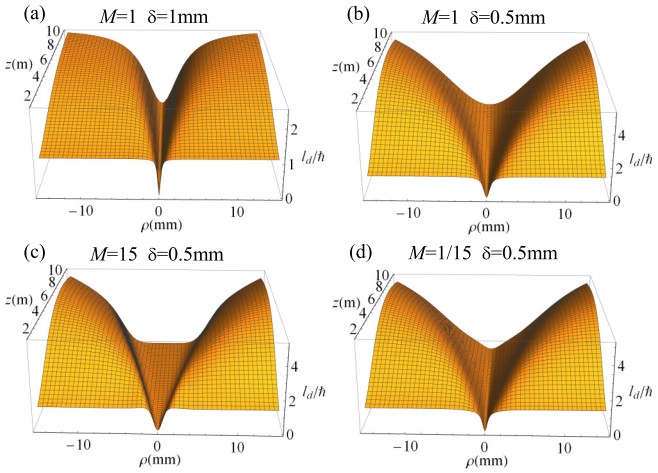

FIG. 1. The normalized OAM flux density of multi-Gaussian Schell-model beams on propagation, for different orders M and different correlation widths δ.

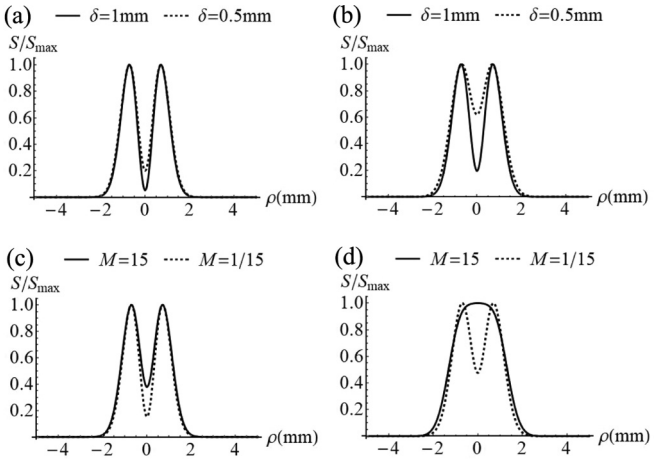

FIG. 3. The normalized spectral density of MGSMV beams at $z = 0.5$ m (a), (c) and $z = 1$ m (b), (d), with $M = 1$ (a), (b) and $\delta = 0.5$ mm (c), (d).

will exhibit this rigid body behavior at a shorter propagation distance. These figures demonstrate how the correlation width dramatically affects the distribution of OAM on propagation.

Figures 1(c) and 1(d) show examples of the normalized OAM flux density for $M > 1$ and $M < 1$; it can be seen that this flux density takes on flat-topped or cusped profiles, respectively. The former case represents an OAM "dead zone" in the center of the beam, in which there is no circulation.

These latter examples, curiously, mimic the spectral density profiles of their respective beams: a beam with a flat-topped spectral density, for instance, results in a flat-bottomed "dead zone" in the OAM. The OAM flux densities and corresponding spectral densities $S(\mathbf{r}) = W(\mathbf{r}, \mathbf{r})$ are illustrated for MGSM beams at a fixed propagation distance in Fig. 2. It is to be noted that the most dramatic changes in the OAM flux density occur in regions where the spectral density

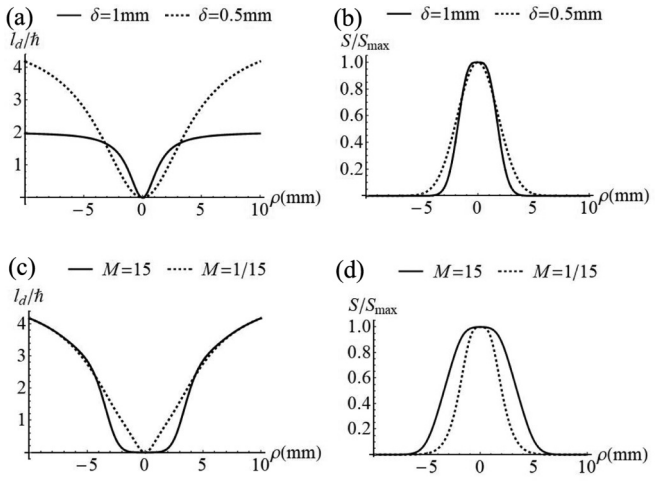

FIG. 2. The normalized OAM flux density and spectral density of MGSMV beams with $M = 1$ and $z = 5$ m (a), (b) and $\delta = 0.5$ mm and $z = 5$ m (c), (d).

is still high: these OAM changes are not confined to regions with few or no photons.

The propagation distances in Fig. 2 were chosen to highlight the most dramatic OAM flux changes; however, this does not clearly show the evolution of the spectral density for the different cases. In Fig. 3 the spectral densities of all cases are shown at $z = 0.5$ and 1.0 m. It can be seen that all beams maintain a low intensity core at short propagation distances, which becomes less prominent and eventually vanishes at large propagation distances. This demonstrates that the OAM flux density changes are not simply an artifact of the distribution of spectral density: the OAM flux density remains low in the beam's core even when the spectral density in the core increases.

Even more extreme changes in the distribution of OAM can be achieved with partial coherence, even the creation of counter-rotating regions. To illustrate this, we consider a source which is an incoherent superposition of GSMV beams with equal and opposite topological charges but different correlation widths δ_n, i.e.,

$$W(\mathbf{r}_1, \mathbf{r}_2) = \sum_{n=+l,-l} U_n^*(\mathbf{r}_1) U_n(\mathbf{r}_2) \exp\left[-\frac{|\mathbf{r}_2 - \mathbf{r}_1|^2}{\delta_n^2}\right]. \quad (13)$$

Because the intensity profiles of the two contributions are the same, $t_d = 0$ and the normalized OAM flux density $l_d(\mathbf{r}) = 0$

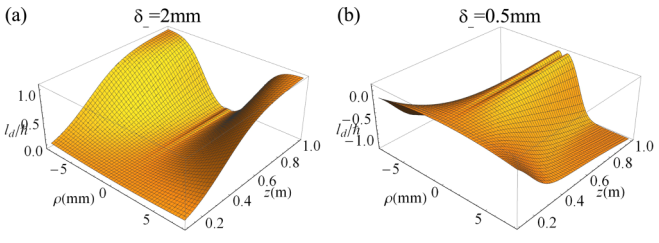

FIG. 4. The normalized OAM flux density of an incoherent superposition of GSMV beams with $|l| = 1$ and $\delta_+ = 1$ mm.

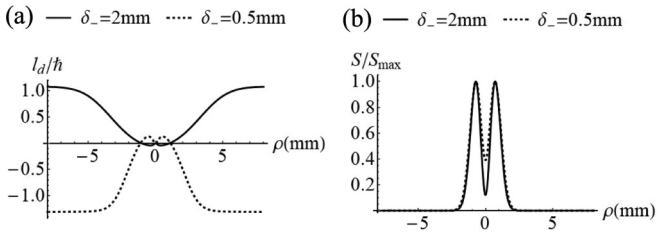

FIG. 5. The (a) normalized OAM flux density and (b) spectral density of an incoherent superposition of GSMV beams with $|l| = 1$, $\delta_+ = 1$ mm, and $z = 1$ m.

in the source plane. But if the correlation widths of the two components are different they will propagate differently, resulting in a nonconstant normalized OAM flux density away from the source. The continuous evolution of $l_d(\mathbf{r})$ as a function of z is shown in Fig. 4, for two different values of δ_-, with $|l| = 1$, $\delta_+ = 1$ mm. For both values of δ_-, one can see a "dent" in the curve near $\rho = 0$. To highlight this, we plot the OAM flux density for several values of δ_- in Fig. 5(a) at $z = 1$ m. We can see that there exist counter-rotating (positive and negative) regions of OAM flux density in the beam when δ_+ and δ_- are significantly different from each other, and that the radial locations of these regions can be "flipped" by changing the value of δ_-. The spectral densities for the examples are shown in Fig. 5(b).

IV. DISCUSSION

It is natural to ask how one might generate and measure these OAM changes experimentally. A source of the form of Eq. (13) is the incoherent superposition of two partially coherent vortex beams. Such beams can be generated from independent lasers and then combined in an optical system. The individual beams can be generated using a pair of digital micromirror devices (DMDs). Alternatively, a single DMD can be used to generate frames which alternate between realizations of the two independent vortex beams; this strategy was discussed in [26] and a description of how to generate the desired realizations is given in [27]. To measure OAM changes, the most straightforward possibility would be to measure the motion of microscopic particles in the path of the beam, deducing the strength and handedness of the rotation by the direction the particle moves. Small particles can be put into orbital motion by OAM beams; this was impressively demonstrated some years ago when microspheres were used in a sequence of counter-rotating vortex beams to create a micro-optomechanical fluid pump [13]. A beam such as that described by Eq. (13), which produces counter-rotating regions from a beam that starts with no net OAM, would provide a clear qualitative indication of correlation-induced OAM changes.

We have therefore demonstrated the existence of correlation-induced OAM changes, which join spectral changes and polarization changes in a family of coherence-influenced propagation phenomena. The examples shown here are illustrative of the phenomenon, but not exhaustive—it is expected that other choices of the source coherence can result in different types of changes, and the creation of more prominent counter-rotating regions. This paper, which highlights a previously unexplored physical phenomenon, also provides an additional degree of freedom for the control and trapping of microscopic particles.

ACKNOWLEDGMENTS

The authors would like to acknowledge the National Key Research and Development Project of China (Grant No. 2019YFA0705000), National Natural Science Foundation of China (Grants No. 11974218, No. 91750201, No. 11525418, and No. 11474143), Innovation Group of Jinan (Grant No. 2018GXRC010), and Local science and technology development project of the central government (No. YDZX20203700001766).

APPENDIX: THE OAM OF A GAUSSIAN SCHELL-MODEL VORTEX BEAM

We evaluate the cross-spectral density and OAM properties of a Gaussian Schell-model partially coherent vortex beam; in the source plane $z = 0$, the cross-spectral density has the form

$$W(\mathbf{r}_1, \mathbf{r}_2) = U_l^*(\mathbf{r}_1) U_l(\mathbf{r}_2) \exp\left[-\frac{|\mathbf{r}_1 - \mathbf{r}_2|^2}{\delta^2}\right], \tag{A1}$$

with $U_l(\mathbf{r})$ given by Eq. (8), and δ represents the correlation width.

The cross-spectral density function of a partially coherent beam after propagating in free space a distance z can be calculated by Fresnel propagation:

$$W(\boldsymbol{\rho}_1, \boldsymbol{\rho}_2, z) = \frac{1}{(\lambda z)^2} \iint W(\mathbf{r}_1, \mathbf{r}_2) \exp\left\{-\frac{ik}{2z}[(\mathbf{r}_1 - \boldsymbol{\rho}_1)^2 - (\mathbf{r}_2 - \boldsymbol{\rho}_2)^2]\right\} d^2 r_1 d^2 r_2. \tag{A2}$$

Substituting from Eq. (A1) into Eq. (A2), the integrals can be evaluated analytically. The result for $l = 1$ is given by

$$W(\boldsymbol{\rho}_1, \boldsymbol{\rho}_2, z) = \frac{|C_1|^2}{\lambda^2 z^2} \frac{\pi^2}{2A_2^2 M^2} \exp\left[-\frac{ik}{2z}\left(\rho_1^2 - \rho_2^2\right)\right] \exp\left[-\frac{k^2 \rho_2^2}{4z^2 A_2} - \frac{k^2}{4z^2 M}\left(\boldsymbol{\rho}_1 - \frac{\boldsymbol{\rho}_2}{A_2 \delta^2}\right)^2\right]$$
$$\times\left[\frac{2}{\delta^2} - \frac{k^2}{2z^2 M \delta^2}\left(\boldsymbol{\rho}_1 - \frac{\boldsymbol{\rho}_2}{A_2 \delta^2}\right)^2 - \frac{k^2}{2z^2}\left(\frac{\rho_2^2}{A_2 \delta^2} - \boldsymbol{\rho}_1^* \cdot \boldsymbol{\rho}_2\right)\right], \tag{A3}$$

with

$$A_1 = \frac{1}{w^2} + \frac{1}{\delta^2} + \frac{ik}{2z}, \tag{A4}$$

$$A_2 = \frac{1}{w^2} + \frac{1}{\delta^2} - \frac{ik}{2z}, \tag{A5}$$

$$M = A_1 - \frac{1}{A_2\delta^4}. \tag{A6}$$

The OAM flux density may then be derived through the use of Eq. (2). On substitution, we find that this flux density is of the form

$$L_d(\boldsymbol{\rho}, z) = \mathrm{Im}\left(\frac{|C_1|^2\pi^2 k\epsilon_0\rho^2}{4\lambda^2 z^4} \frac{i}{A^2M^2} \exp\left\{ -\frac{k^2\rho^2}{4z^2}\left[\frac{1}{A_2} + \frac{1}{M}\left(1 - \frac{1}{A_2\delta^2}\right)^2 \right] \right\} \right). \tag{A7}$$

With this formula, the normalized OAM flux density can be calculated using Eq. (3).

The other two examples in the paper, MGSMV beams and the incoherent superposition beam, can be constructed by superpositions of the solution above with different widths δ.

[1] E. Collett and E. Wolf, Is complete spatial coherence necessary for the generation of highly directional light beams?, Opt. Lett. **2**, 27 (1978).

[2] E. Wolf, Invariance of the Spectrum of Light on Propagation, Phys. Rev. Lett. **56**, 1370 (1986).

[3] Z. Dačić and E.Wolf, Changes in the spectrum of partially coherent light beam propagating in free space, J. Opt. Soc. Am. A **5**, 1118 (1988).

[4] E. Wolf, Non-cosmological redshifts of spectral lines, Nature (London) **326**, 363 (1987).

[5] D. F. V. James, Change of polarization of light beams on propagation in free space, J. Opt. Soc. Am. A **11**, 1641 (1994).

[6] O. Korotkova and E. Wolf, Changes in the state of polarization of a random electromagnetic beam on propagation, Opt. Commun. **246**, 35 (2005).

[7] M. S. Soskin and M. V. Vasnetsov, Singular optics, Prog. Opt. **42**, 219 (2001).

[8] M. R. Dennis, K. O'Holleran, and M. J. Padgett, Singular optics: Optical vortices and polarization singularities, in *Progress in Optics*, Vol. 53 (Elsevier, Amsterdam, 2009), pp. 293–363.

[9] G. Gbur, *Singular Optics* (CRC, Boca Raton, FL, 2016).

[10] L. Allen, M. W. Beijersbergen, R. J. C. Spreeuw, and J. P. Woerdman, Orbital angular momentum of light and the transformation of Laguerre-Gaussian laser modes, Phys. Rev. A **45**, 8185 (1992).

[11] *Optical Angular Momentum*, edited by L. Allen, S. M. Barnett, and M. J. Padgett (IOP, Bristol, 2003).

[12] N. B. Simpson, K. Dholakia, L. Allen, and M. J. Padgett, Mechanical equivalence of spin and orbital angular momentum of light: An optical spanner, Opt. Lett. **22**, 52 (1997).

[13] K. Ladavac and D. G. Grier, Microoptomechanical pumps assembled and driven by holographic optical vortex arrays, Opt. Express **12**, 1144 (2004).

[14] G. Gibson, J. Courtial, M. J. Padgett, M. Vasnetsov, V. Pas'ko, S. M. Barnett, and S. Franke-Arnold, Free-space information transfer using light beams carrying orbital angular momentum, Opt. Express **12**, 5448 (2004).

[15] J. Wang, J.-Y. Yang, I. M. Fazal, N. Ahmed, Y. Yan, H. Huang, Y. Ren, Y. Yue, S. Dolinar, M. Tur, and A. E. Willner, Terabit free-space data transmission employing orbital angular momentum multiplexing, Nat. Photonics **6**, 488 (2012).

[16] G. Gbur and T. D. Visser, Coherence vortices in partially coherent beams, Opt. Commun. **222**, 117 (2003).

[17] G. Gbur, T. D. Visser, and E. Wolf, "Hidden" singularities in partially coherent wavefields, J. Opt. A: Pure Appl. Opt. **6**, S239 (2004).

[18] D. M. Palacios, I. D. Maleev, A. S. Marathay, and G. A. Swartzlander, Jr., Spatial Correlation Singularity of a Vortex Field, Phys. Rev. Lett. **92**, 143905 (2004).

[19] S. M. Kim and G. Gbur, Angular momentum conservation in partially coherent wave fields, Phys. Rev. A **86**, 043814 (2012).

[20] G. A. Swartzlander, Jr. and R. I. Hernandez-Aranda, Optical Rankine Vortex and Anomalous Circulation of Light, Phys. Rev. Lett. **99**, 163901 (2007).

[21] G. Gbur, Partially coherent vortex beams, in *Complex Light and Optical Forces XII, Proc. SPIE* 10549, edited by E. J. Galvez, D. L. Andrews, and J. Glückstad (SPIE, Bellingham, WA, 2018), p. 1054903.

[22] S. Sahin and O. Korotkova, Light sources generating far fields with tunable flat profiles, Opt. Lett. **37**, 2970 (2012).

[23] O. Korotkova and X. Chen, Phase structuring of complex degree of coherence, Opt. Lett. **43**, 4727 (2018).

[24] E. Wolf, *Introduction to the Theory of Coherence and Polarization of Light* (Cambridge University, Cambridge, England, 2007).

[25] F. Wang and O. Korotkova, Circularly symmetric cusped random beams in free space and atmospheric turbulence, Opt. Express **25**, 5057 (2017).

[26] X. Chen, J. Li, S. Rafsanjani, and O. Korotkova, Synthesis of I_0-Bessel-correlated beams via coherent modes, Opt. Lett. **43**, 3590 (2018).

[27] M. Hyde, S. Basu, D. Voelz, and X. Xiao, Experimentally generating any desired partially coherent Schell-model source using phase-only control, J. Appl. Phys. **118**, 093102 (2015).